

# The effect of nanometre-sized Au particle loading on TiO<sub>2</sub> photocatalysed reduction of bis(2-dipyridyl)disulfide to 2-mercaptopyridine by H<sub>2</sub>O†

Hiroaki Tada,<sup>\*a</sup> Fumiaki Suzuki,<sup>b</sup> Shigeki Yoneda,<sup>b</sup> Seishiro Ito<sup>b,a</sup> and Hisayoshi Kobayashi<sup>c</sup>

<sup>a</sup> Molecular Engineering Institute, Kinki University, 3-4-1, Kowakae, Higashi-Osaka, Osaka 577-8502, Japan. E-mail: h-tada@apsrv.apch.kindai.ac.jp

<sup>b</sup> Department of Applied Chemistry, Faculty of Science and Engineering, Kinki University, 3-4-1, Kowakae, Higashi-Osaka, Osaka 577-8502, Japan

<sup>c</sup> Department of Chemical Technology, Kurashiki University of Science and Arts, 2640 Nishinoura, Tsurajima, Kurashiki 712, Japan

Received 26th September 2000, Accepted 6th February 2001

First published as an Advance Article on the web 7th March 2001

TiO<sub>2</sub> photocatalysed reduction of bis(2-dipyridyl)disulfide (RSSR) to 2-mercaptopyridine by H<sub>2</sub>O is enhanced significantly by incorporation of nanometre-sized Au particles. The rate is strongly dependent on the amount of Au loaded (*x* wt.%), passing through a maximum at *x* ~ 0.3, while it is almost independent of the Au particle size in the 4.3–11 nm range. Comparison of the effects of Au and Ag loading reveals that the rate constant of the Au(0.25 wt.%)/TiO<sub>2</sub> system is greater than that of the Ag(0.24 wt.%)/TiO<sub>2</sub> system by a factor of 2.6 and the activation energy of the former is about two-thirds that of the latter. The enhancing effect of the Au loading is discussed in terms of kinetic and molecular orbital considerations.

## Introduction

In TiO<sub>2</sub> photocatalysis, both oxidation and reduction, derived respectively from the valence band hole ( $h_{vb}^+$ ) and the conduction band electron ( $e_{cb}^-$ ), proceed simultaneously on the TiO<sub>2</sub> surface. A great deal of research, including the application to air and water purification, has focused on the oxidation process owing to the strong oxidizing power of the  $h_{vb}^+$ .<sup>1</sup> Much less attention has been paid to the reductive photochemistry of TiO<sub>2</sub> because of the moderate reducing power of the  $e_{cb}^-$ .<sup>2–8</sup> We have recently reported that bis(2-dipyridyl)disulfide (RSSR) is reduced to 2-mercaptopyridine (RSH) by H<sub>2</sub>O using TiO<sub>2</sub> as a photocatalyst and that the rate is enhanced by loading the TiO<sub>2</sub> with Ag nanoclusters.<sup>9</sup> This efficient endothermic reaction is attractive from the viewpoint of converting light energy to chemical energy as well as yielding thiols that are the starting materials for many useful products.<sup>10</sup> It was also suggested that the rise in the Fermi energy of TiO<sub>2</sub> with photoirradiation is essential for the photocatalytic cycle.<sup>9</sup>

Various self-assembled monolayers (SAMs) of organosulfur compounds on Au or Ag surfaces have been studied in the field of surface science.<sup>11</sup> It has been well established by vibrational spectroscopy that the structures of SAMs of *n*-alkanethiols formed on Au(111) and Ag(111) surfaces are quite similar except for the tilt angle  $\theta$  ( $\theta(\text{Au}) \sim 30^\circ$ ,  $\theta(\text{Ag}) \sim 6^\circ$ ).<sup>11</sup> Although both Au and Ag with an equivalent electronic configuration ( $ns^2np^6nd^{10}(n+1)s$ ) belong to Group 11 of the periodic table, the work function and the oxidation potential of Au are greater than those of Ag.

This is the first report on a marked Au enhancing effect exceeding that of Ag on the TiO<sub>2</sub> photocatalytic reduction of RSSR to RSH by H<sub>2</sub>O. The mode of action of the nanometre-

sized Au particles is discussed on the basis of the reaction mechanism proposed.

## Experimental

### Materials

Anatase TiO<sub>2</sub> particles were supplied by Ishihara Techno Co. (A-100) and used without further activation. The specific surface area ( $S/m^2 g^{-1}$ ) was determined to be  $8.1 m^2 g^{-1}$  from N<sub>2</sub> gas adsorption at  $-196^\circ C$  based on the BET equation. Water was used after being passed through an ion-exchange resin.

A KI–I<sub>2</sub> aqueous solution was added dropwise to a solution of 2-mercaptopyridine (40.4 g, 360 mmol, >95%, Tokyo Kasei) in a 2 M aqueous solution of NaOH (500 mL) until the reaction mixture turned brown. To this solution was added an aqueous solution of Na<sub>2</sub>S<sub>2</sub>O<sub>3</sub> followed by extraction with benzene (200 mL) three times. The benzene layer was washed with water and dried over MgSO<sub>4</sub>. After the solvent had been evaporated, the residue was purified by recrystallization from a mixed solvent of *n*-hexane and benzene to yield bis(2-dipyridyl)disulfide: Yield: 72%, mp: 57–58 °C, <sup>1</sup>H NMR (60 MHz, CDCl<sub>3</sub>,  $\delta$  ppm); 7.03–7.50 (m, 3Py, 3'Py, 5Py, 5'Py 4H), 8.57 (d, 4Py, 4'Py, 2H), 8.60 (d, 6Py, 6'Py, 2H).<sup>12</sup> The other reagents were used as received.

### Preparation of photocatalysts

Nanometre-sized Au particles were deposited on the surface of TiO<sub>2</sub> by the deposition–precipitation method.<sup>13</sup> After the pH of a  $4.86 \times 10^{-3}$  M aqueous solution (100 mL) of HAuCl<sub>4</sub>·4H<sub>2</sub>O (Kishida Chemicals, >99.3%) had been adjusted to 6.0 with 0.4 M NaOH, TiO<sub>2</sub> particles (10 g) were suspended with stirring at 70 °C for 1 h. The particles were washed with distilled water three times and kept under vacuum at room temperature. The dried particles were calcined at 400 or 600 °C for 4 h in air in an electric oven. TiO<sub>2</sub>

† Electronic Supplementary Information available. See <http://www.rsc.org/suppdata/cp/b0/b007817o>

particles loaded with nanometre-sized Ag particles (Ag/TiO<sub>2</sub>) were prepared by the photodeposition method described in an earlier paper.<sup>9</sup> The Au and Ag deposits on TiO<sub>2</sub> were dissolved by treating the particles (1 g) with *aqua regia* (50 mL) and HNO<sub>3</sub> (13.5 M, 50 mL), respectively. The resultant aqueous Au<sup>3+</sup> and Ag<sup>+</sup> solutions were subjected to inductively coupled plasma spectroscopy (ICPS-1000, Shimadzu); the catalysts loaded with *x* wt.% Au and Ag were denoted as Au(*x* wt.%)/TiO<sub>2</sub> and Ag(*x* wt.%)/TiO<sub>2</sub>, respectively. The size and distribution of Au particles deposited on TiO<sub>2</sub> were directly observed by a transmission electron microscope (JEOL, JEM-3010) at an acceleration voltage of 300 kV and a current of 115 μA.

### Photocatalytic reduction of 2,2'-RSSR

The photoreaction solution of RSSR ( $5.41 \times 10^{-5}$  M) was prepared by diluting an acetonitrile solution ( $5.41 \times 10^{-4}$  M) with H<sub>2</sub>O (acetonitrile : H<sub>2</sub>O = 1 : 99 v/v). After the suspension of TiO<sub>2</sub> or Au/TiO<sub>2</sub> or Ag/TiO<sub>2</sub> had been purged with N<sub>2</sub> for 15 min, irradiation was started in a double jacket type reaction cell (31 mm in diameter and 175 mm in length, transparent to light with  $\lambda > 300$  nm). The light intensity integrated from 320 to 400 nm ( $I_{320-400}$ ) was measured using a digital radiometer (DRC-100X, Spectroline). N<sub>2</sub> gas bubbling (6.1 mL min<sup>-1</sup>) and magnetic stirring of the suspension were continued throughout the irradiation. The cell was kept at various steady temperatures (10–50 °C) by circulating thermostatted water through an outer jacket around the cell. The pH of the suspension was adjusted by adding a 0.1 M aqueous solution of NaOH or HCl.

Electronic absorption spectra of the supernatants obtained by centrifugation of the suspensions after irradiation were recorded in the 200–500 nm range on an ultraviolet–visible spectrophotometer (U-4000, Hitachi). The concentrations of RSSR consumed and RSH generated were determined from the absorbance at 281 ( $\epsilon_{\max} = 1.05 \times 10^4$  M<sup>-1</sup> cm<sup>-1</sup>) and 342 nm ( $\epsilon_{\max} = 7.18 \times 10^3$  M<sup>-1</sup> cm<sup>-1</sup>), respectively. The initial rate of the reaction (*v*) was calculated from the concentration of RSH (*C*) generated after 20 min irradiation ( $v = C/20$ ).

Product analysis was performed separately by high performance liquid chromatography (HPLC) [HPLC measurement conditions: column = Fluorofix INW 425 4.6 × 250 mm (NEOS); mobile phase H<sub>2</sub>O–MeOH (1/1 v/v); flow rate = 1 mL min<sup>-1</sup>].

Adsorption isotherms of RSSR at  $25 \pm 1$  °C were obtained by exposing the catalysts to solutions of varying concentrations for 24 h in the dark followed by centrifugation and spectrophotometric analysis of the RSSR remaining in the solution. Analysis of O<sub>2</sub> was attempted in a closed reaction system, where the dissolved O<sub>2</sub> had been purged with Ar before irradiation, by gas chromatography using a Shimadzu GC-8APT equipped with a t.c.d. column SHINCARBON T (6 m × 2 mm), Ar carrier at 50 °C.

## Results and discussion

### Characterization of photocatalysts

Fig. 1 shows TEM micrographs of Au/TiO<sub>2</sub> particles. In each sample, nanometre-sized Au particles are uniformly dispersed

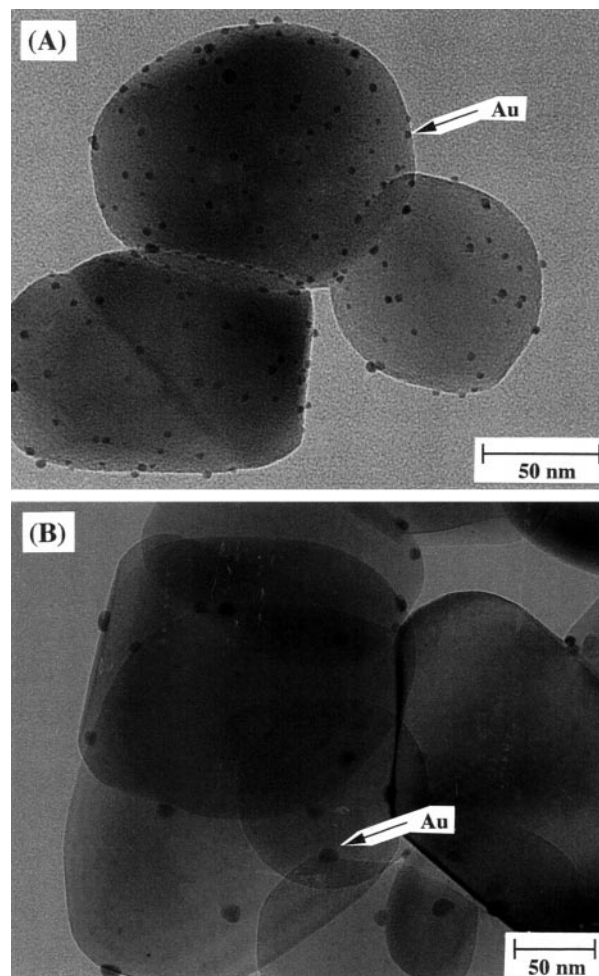


Fig. 1 TEM micrographs of Au/TiO<sub>2</sub> particles (A,  $T_c = 673$  K; B,  $T_c = 873$  K).

on the surface of TiO<sub>2</sub> by the deposition–precipitation method. Fig. 2 shows the size distributions of Au particles loaded on the TiO<sub>2</sub>. An increase in the calcination temperature  $T_c$  from 673 to 873 K leads to a significant increase in the average diameter (*d*) of the Au particles from 4.3 to 11 nm concurrently with a decrease in their number density (Fig. 1). Also, the size distribution in the sample with  $T_c = 673$  K is narrower than that in the sample with  $T_c = 873$  K. The Au particles are considered as coalescing to grow upon heating at  $T_c > 673$  K. The Au/TiO<sub>2</sub> and Ag/TiO<sub>2</sub> samples had a surface plasmon absorption due to nanometre-sized metal deposits in the visible region. A small red shift ( $\Delta\lambda = 5.4$  nm) of the peak maximum ( $\lambda_{\max}$ ) of the Au/TiO<sub>2</sub> with increasing  $T_c$  can be attributed to an increase in *d*.<sup>14</sup> Table 1 summarizes some physicochemical properties of Au/TiO<sub>2</sub> and Ag/TiO<sub>2</sub>. Only the size of the Au particle can be changed with  $T_c$ , while both *x* and *S* remain almost constant.<sup>15</sup>

### Adsorption

Fig. 3A shows adsorption isotherms of RSSR on TiO<sub>2</sub> (a) and Au(0.35 wt.%)/TiO<sub>2</sub> (b) at  $25 \pm 1$  °C;  $C_{\text{eq}}/\text{M}$  and  $\Gamma/\text{mol g}^{-1}$

Table 1 Results of characterization of Ag/TiO<sub>2</sub> and Au/TiO<sub>2</sub>

Photocatalyst	Method	$T_c/\text{K}$	<i>x</i> (wt.%)	<i>d</i> /nm <sup>a</sup>	$\lambda_{\max}/\text{nm}^a$	<i>S</i> /m <sup>2</sup> g <sup>-1</sup>
Ag/TiO <sub>2</sub>	p.d. <sup>b</sup>	—	0.24	<5.0	495.0	6.8
Au/TiO <sub>2</sub>	d.p. <sup>b</sup>	673	0.25 ± 0.03	4.3	542.8	9.4
Au/TiO <sub>2</sub>	d.p.	873	0.25 ± 0.03	11	548.2	9.6

<sup>a</sup> *d* and  $\lambda_{\max}$  are the average diameter of metals deposited and the peak wavelength of the surface plasmon absorption, respectively. <sup>b</sup> p.d. and d.p. denote photodeposition and deposition–precipitation, respectively.

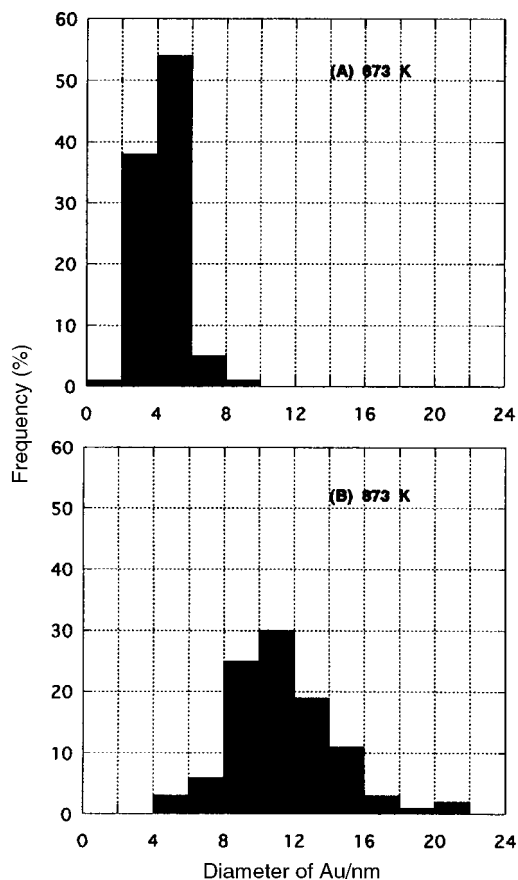


Fig. 2 Size distributions of Au particles loaded on TiO<sub>2</sub> (A,  $T_c = 673$  K; B,  $T_c = 873$  K).

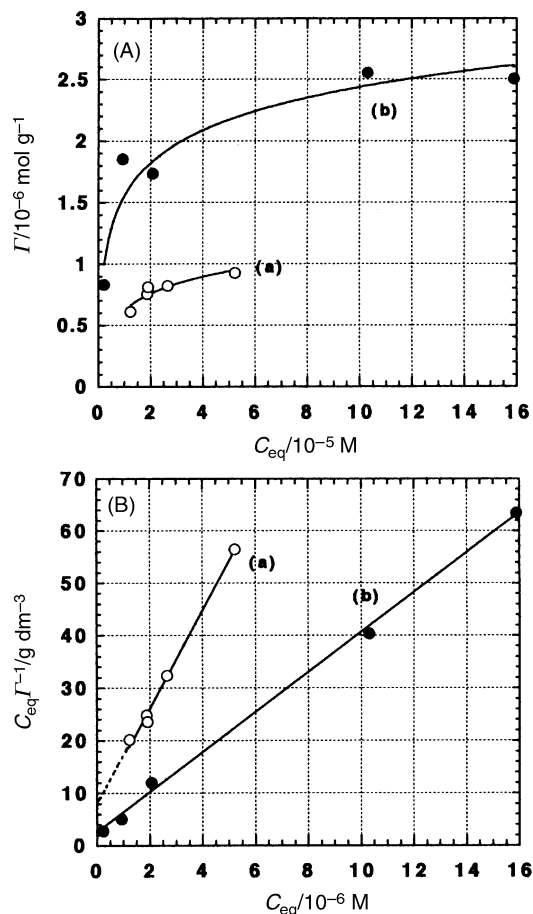


Fig. 3 A, Adsorption isotherms of RSSR on TiO<sub>2</sub> (a) and Au(0.35 wt.)/TiO<sub>2</sub> (b) at  $25 \pm 1$  °C. B, Langmuir's plots for the TiO<sub>2</sub> (a) and Au(0.35 wt.)/TiO<sub>2</sub> (b) systems.

are the equilibrium concentration and the adsorption amount, respectively. A significant increase in the adsorption amount of RSSR is seen in Au(0.35 wt.)/TiO<sub>2</sub> as compared to TiO<sub>2</sub>. As shown in Fig. 3B, the adsorption behavior in each system obeys the Langmuir model. From the slopes of the straight lines ((a)  $R = 0.997$ ; (b)  $R = 0.998$ ), the saturated adsorption amounts ( $\Gamma_s/\text{mol g}^{-1}$ ) were calculated to be  $1.07 \times 10^{-6} \text{ mol g}^{-1}$  for TiO<sub>2</sub> and  $2.63 \times 10^{-6} \text{ mol g}^{-1}$  for Au(0.35 wt.)/TiO<sub>2</sub>. Disulfides are known to chemisorb on Au(111) or Ag(111) surfaces *via* S–S bond cleavage.<sup>16</sup> Gui *et al.* confirmed that the RS groups adsorb stably on Ag without S–C bond fission,<sup>17</sup> which was observed in R'SR' adsorption on Au(111) ( $R'$  = organic groups).<sup>18</sup> The areas occupied by one RS group on the Au(0.35 wt.)/TiO<sub>2</sub> particle were calculated to be  $6.4 \text{ nm}^2 \text{ group}^{-1}$  on the TiO<sub>2</sub> part ( $\sigma(\text{TiO}_2)$ ) and  $0.07 \text{ nm}^2 \text{ group}^{-1}$  on the Au part ( $\sigma(\text{Au})$ ). The values of  $\sigma$  for the RS group adsorbed in the closest packing states were estimated to be *ca.*  $0.16 \text{ nm}^2 \text{ group}^{-1}$  for the flat lying orientation and *ca.*  $0.1 \text{ nm}^2 \text{ group}^{-1}$  for the vertical orientation using the PM3 optimized molecular structure.<sup>19</sup> Clearly, the RS groups adsorb selectively on the surface of nanometre-sized Au particles in a close packed state. The same was concluded previously for the Ag/TiO<sub>2</sub> system.<sup>19</sup>

### Photocatalytic reduction

TiO<sub>2</sub> and Au/TiO<sub>2</sub> absorb light intensely below 385 nm due to the band gap transition of TiO<sub>2</sub>. Au/TiO<sub>2</sub> particles have a surface plasmon absorption peak around 545 nm. In the spectrum of RSSR, there are two absorption bands above 220 nm, at 233 (B<sub>1</sub>) and 281 nm (B<sub>2</sub>). A Pyrex glass filter removed light of  $\lambda < 300$  nm, and both TiO<sub>2</sub> and Au were excited by the irradiation. Fig. 4 shows the change in the electronic absorption spectrum of RSSR with irradiation in the presence of Au(0.25 wt.)/TiO<sub>2</sub>. As time increases, the peak intensities of B<sub>1</sub> and B<sub>2</sub> weaken and two new bands appear at 272 (B<sub>3</sub>) and 342 nm (B<sub>4</sub>). These peak positions are in complete agreement with those of an authentic 2-mercaptopyridine (RSH) sample. As shown in the inset, a stoichiometric ratio of [RSH]/[RSSR] of *ca.* 2 is obtained, indicating selective reduction of RSSR to RSH. This was further confirmed, by HPLC analysis.† UV irradiation of either Au/TiO<sub>2</sub> or TiO<sub>2</sub> was

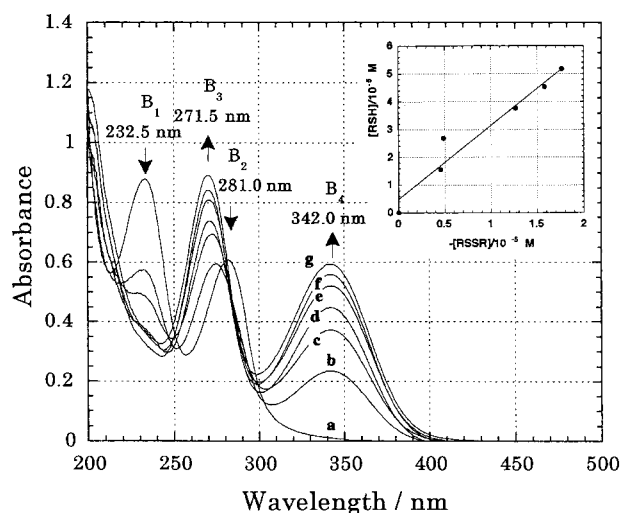
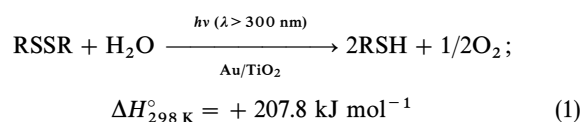


Fig. 4 Change in the electronic absorption spectrum of a  $5.41 \times 10^{-5} \text{ M}$  RSSR solution (50 mL of a mixed solvent of H<sub>2</sub>O: acetonitrile = 99 : 1 v/v) with photoirradiation ( $\lambda > 300$  nm) in the presence of Au(0.25 wt.)/TiO<sub>2</sub> (50 mg) at  $30 \pm 0.5$  °C: a, irradiation time ( $t/\text{min}$ ) = 0; b, 20; c, 40; d, 60; e, 80; f, 100; g, 120. The  $I_{320-400}$  was  $4.6 \text{ mW cm}^{-2}$ . Irradiation was started after removal of the dissolved O<sub>2</sub> by 15 min N<sub>2</sub> bubbling. N<sub>2</sub> bubbling was continued throughout the reaction. The inset shows the stoichiometric relation in the conversion of RSSR to RSH.

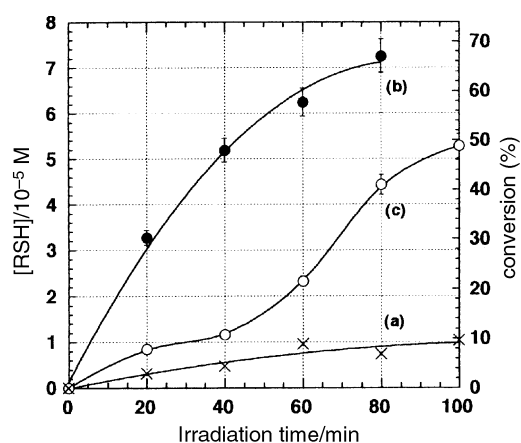
needed to reduce RSSR. This suggests that the reaction is induced not by photoexcitation of Au, *i.e.*, the hot-electron mechanism,<sup>20</sup> but by the band gap transition of TiO<sub>2</sub>. A gradual decrease in pH with increasing *t* is evidence for the generation of H<sup>+</sup> during the oxidation of adsorbed H<sub>2</sub>O by the holes. Analysis of O<sub>2</sub> was attempted in a closed reaction system, where the dissolved O<sub>2</sub> had been purged with Ar before irradiation. Although the quantity could not be precisely determined, a small amount of O<sub>2</sub> was detected. Evidently, the oxidation of H<sub>2</sub>O to O<sub>2</sub> and H<sup>+</sup> occurs simultaneously with the reduction of RSSR to RSH. The overall reaction can be written as eqn. (1), where the oxidation number of O increases from -2 to 0 and that of S decreases from 0 to -1.



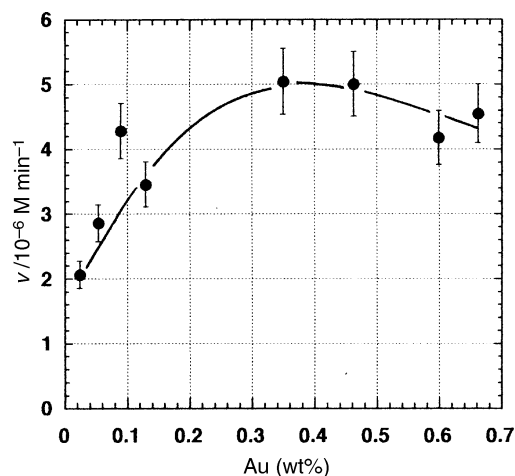
The low level of O<sub>2</sub> detected during the reaction is probably due to its consumption through successive reduction by the excited electron and/or reaction with RSSR.<sup>21</sup> Peroxide formation on the surface of TiO<sub>2</sub> may also make a contribution.<sup>22</sup> The possibility of the oxidation of acetonitrile was excluded, because no reduction of RSSR occurred upon using 100% dehydrated acetonitrile as solvent.

Fig. 5 shows the time courses of RSH formation in the presence of TiO<sub>2</sub> (a), Au(0.25 wt.)/TiO<sub>2</sub> (b), and Ag(0.24 wt.)/TiO<sub>2</sub> (c) at 30.0 ± 0.5 °C. In each case, the amount of RSH increases monotonically with increasing *t*. The enhancing effect of the Au loading is much greater than of the Ag loading at comparable amounts of metal loading. The conversion of RSSR to RSH after 80 min illumination attains *ca.* 67% in system (b), while it is 9.6% after 100 min illumination in system (a). In system (c), the reaction has an induction period, and the rate increases steeply at *t* > 40 min. This is probably because the excited electrons are initially used for the reduction of a natural oxide layer formed on the surface of Ag. Such a trend is not observed for Au which has great resistance to surface oxidation.

Haruta *et al.* found the presence of a critical size of Au (*d<sub>c</sub>*) in its catalytic oxidation of CO, where the rate per one surface atom (turnover frequency) increases remarkably at *d* < 5 nm (*d<sub>c</sub>* ≈ 5 nm).<sup>23</sup> In the present system, however, no significant change was observed in the initial rate (*v*) with decreasing *d* from 11 nm (*v* = 1.4 × 10<sup>-6</sup> M min<sup>-1</sup>) to 4.3 nm (*v* = 1.6 × 10<sup>-6</sup> M min<sup>-1</sup>). Fig. 6 shows the dependence of *v* on *x*. The value of *v* increases with increasing *x* at *x* < 0.3,



**Fig. 5** Time courses of RSH formation in the presence of (a) TiO<sub>2</sub> (50 mg (50 mL)<sup>-1</sup>), (b) Au(0.25 wt.)/TiO<sub>2</sub> (50 mg (50 mL)<sup>-1</sup>) and (c) Ag(0.24 wt.)/TiO<sub>2</sub> (50 mg (50 mL)<sup>-1</sup>) at 30.0 ± 0.5 °C. The solvent was a mixture of acetonitrile and H<sub>2</sub>O (1 : 99 v/v). The *I*<sub>320–400</sub> was 4.6 mW cm<sup>-2</sup>.

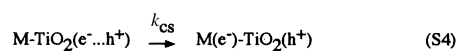
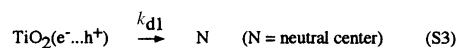


**Fig. 6** The relation between the rate of reaction (*v*) and the amount of Au deposited (*x* wt.%). The reaction temperature was 30 ± 1 °C, and a mixture of acetonitrile and H<sub>2</sub>O (1 : 99 v/v) was used as the solvent. The concentration of the catalyst was 50 mg (50 mL)<sup>-1</sup>. The *I*<sub>320–400</sub> was 4.62 mW cm<sup>-2</sup>.

passing through a maximum at *x* ~ 0.35 wt.%. Since the broad surface plasmon absorption band of Au particles partially overlaps with the absorption band due to the band gap transition of TiO<sub>2</sub>, the decrease in *v* at *x* > 0.45 may be caused by the light shielding action of Au. Another possible reason is the increase in the probability of the recombination of photogenerated charge carriers.<sup>24</sup> The presence of an optimal amount of metal loaded (*x* ~ 0.24 wt.%) was also observed in the Ag/TiO<sub>2</sub> system.<sup>19</sup>

### Mechanism

In an earlier paper, a plausible reaction mechanism was proposed for the Ag/TiO<sub>2</sub> photocatalytic reduction of RSSR.<sup>19</sup> Essentially, the same mechanism seems to be true also for the Au/TiO<sub>2</sub> system (Scheme 1). The selective RSSR adsorption on the surface of metals (M) accompanied by S–S bond cleavage takes place in the initial stage of the reaction (step 1; *K<sub>a</sub>* is the adsorption equilibrium constant). Electron (e<sup>-</sup>)·hole (h<sup>+</sup>) pairs are generated by the band gap excitation of TiO<sub>2</sub> (step 2; *Iφ* is the rate of e<sup>-</sup>·h<sup>+</sup> pair formation). Most of the pairs are lost by recombination (step 3; *k<sub>d1</sub>* is the rate constant of recombination). A portion of the e<sub>cb</sub><sup>-</sup> flows into Au (or Ag), while the h<sub>vb</sub><sup>+</sup> is left in the valence band (VB) of TiO<sub>2</sub> (step 4; *k<sub>cs</sub>* is the rate constant of the charge separation process). Recombination will occur even after the e<sub>cb</sub><sup>-</sup> flow into the metal (step 5; *k<sub>d2</sub>* is the rate constant). The holes have



**Scheme 1** A proposed reaction mechanism in the Au/TiO<sub>2</sub> (or Ag/TiO<sub>2</sub>) system.

a potential positive enough to oxidize  $\text{H}_2\text{O}$  to  $\text{H}^+$  and  $\text{O}_2$  (step 6;  $k_0$  is the rate constant of the oxidation by the hole).<sup>25</sup> The coupling of  $\text{H}^+$  and  $\text{RS}^-$  forms  $\text{RSH}$  (step 7;  $k_r$  is the rate constant of the coupling of  $\text{RS}^-$  and  $\text{H}^+$ ).<sup>26</sup> Application of the steady state approximation to this reaction scheme leads to eqn. (2).

$$d[\text{RSH}]/dt = k[\text{RSSR}]^{1/2} \quad (2)$$

where

$$k = K_a^{1/2} I \phi [k_{cs}/(k_{d1} + k_{cs})][\text{M}/\text{TiO}_2]^{1/2} \times [k_0[\text{H}_2\text{O}_{ad}]^{1/2}/(k_{d2} + k_0[\text{H}_2\text{O}_{ad}]^{1/2})][\text{H}^+] \quad (3)$$

Using the relation  $[\text{RSSR}] = [\text{RSSR}]_0 - [\text{RSH}]/2$ , one can obtain eqn. (4).

$$d[\text{RSH}]/dt = k/\sqrt{2}([2[\text{RSSR}]_0 - [\text{RSH}])^{1/2}} \quad (4)$$

Integration of eqn. (4) from  $t = 0$  to  $t = t$  gives eqn. (5)

$$([2[\text{RSSR}]_0 - [\text{RSH}])^{1/2} = - (k/2\sqrt{2})t + ([2[\text{RSSR}]_0]^{1/2}) \quad (5)$$

Fig. 7 shows plots of  $(C_0 - C)^{1/2}$  vs. irradiation time ( $t$ ) at  $30.0 \pm 0.5^\circ\text{C}$ , where  $C_0$  is twice the initial concentration of RSSR and  $C$  is the concentration of RSH after  $t$  min illumination. The good linearity of each plot supports the validity of the reaction mechanism proposed. The slopes of the straight lines yielded the apparent rate constants ( $k/\text{M}^{1/2} \text{min}^{-1}$ ):  $1.3 \times 10^{-5}$  (a),  $1.5 \times 10^{-4}$  (b) and  $5.9 \times 10^{-5}$  (c). Fig. 8A shows the dependence of  $k$  on reaction temperature ( $T$ ) for (b) Au(0.25 wt.%) $\text{TiO}_2$  and (c) Ag(0.24 wt.%) $\text{TiO}_2$ . In both systems,  $k$  increases exponentially with increasing  $T$ . A reaction-promoting effect of the Au loading exceeding that of the Ag loading is evident over the whole temperature range tested ( $283 < T/\text{K} < 323$ ). Fig. 8B shows the Arrhenius plots of  $\ln k$  vs.  $1000/T$  for Au(0.25 wt.%) $\text{TiO}_2$  (b) and Ag(0.24 wt.%) $\text{TiO}_2$  (c). The activation energies ( $E_a$ ) of systems (b) and (c) were calculated to be 19.7 and 29.4  $\text{kJ mol}^{-1}$ , respectively. The kinetic parameters obtained are summarized in Table 2. The value of  $k$  for Au(0.25 wt.%) $\text{TiO}_2$  is 2.6 times greater

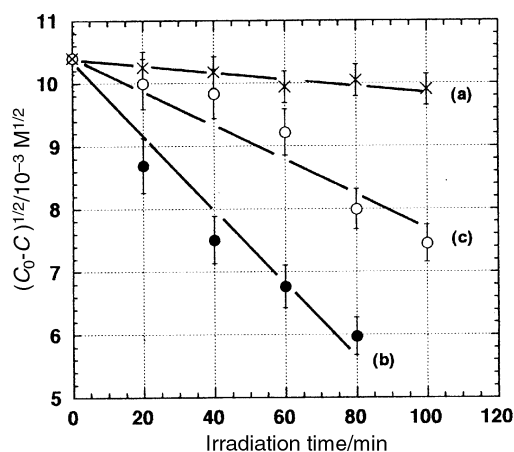


**Fig. 7** Plots of  $(C_0 - C)^{1/2}$  vs. irradiation time ( $t$ ) at  $30.0 \pm 0.5^\circ\text{C}$ ;  $C_0$  is twice the initial concentration of RSSR and  $C$  is the concentration of RSH after  $t$  min illumination. (a),  $\text{TiO}_2$  ( $50 \text{ mg (50 mL)}^{-1}$ ); (b), Au(0.25 wt.%) $\text{TiO}_2$  ( $20 \text{ mg (50 mL)}^{-1}$ ); (c), Ag(0.24 wt.%) $\text{TiO}_2$  ( $50 \text{ mg (50 mL)}^{-1}$ ). The  $I_{320-400}$  was  $4.6 \text{ mW cm}^{-2}$ .

**Table 2** Rate constants and activation energies in the photocatalytic reduction of RSSR

Photocatalyst	Metal loaded (wt.%)	$k/10^{-5} \text{ M}^{1/2} \text{ min}^{-1}$	$E_a/\text{kJ mol}^{-1}$
Au/ $\text{TiO}_2$ <sup>a</sup>	$0.25 \pm 0.03$	15.3	19.7
Ag/ $\text{TiO}_2$	0.24	5.9	29.4
$\text{TiO}_2$	—	1.3	30.6

<sup>a</sup> Annealing temperature was 673 K.

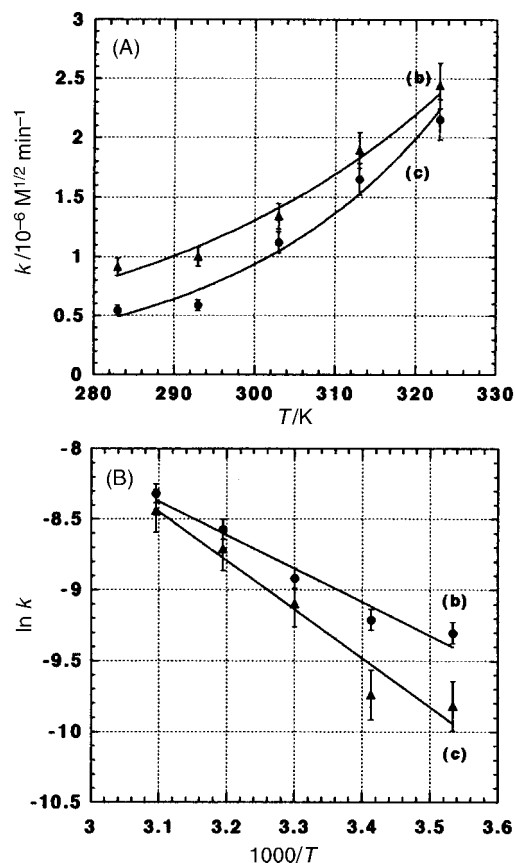
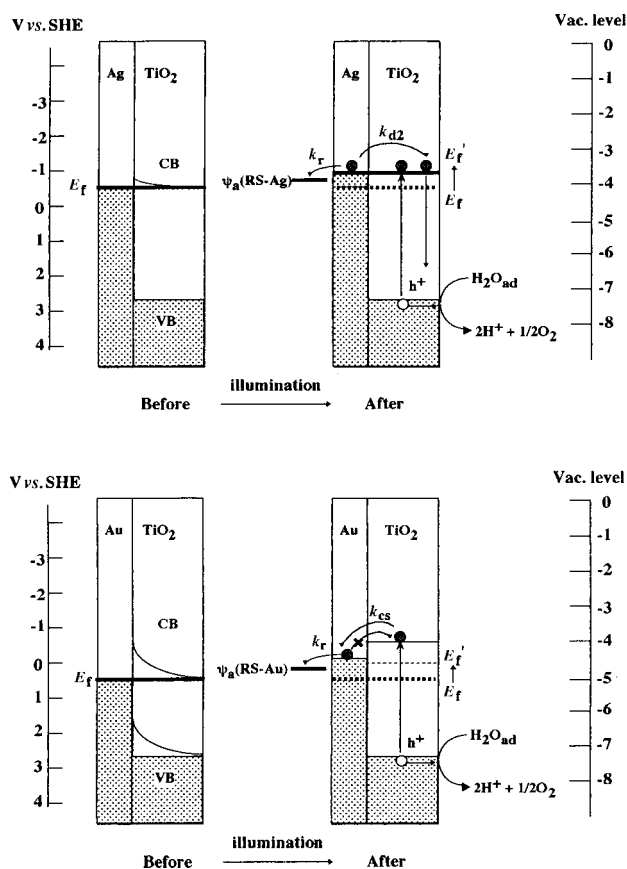


**Fig. 8** A, The reaction temperature ( $T$ ) dependence of  $k$ ; (b), Au(0.25 wt.%) $\text{TiO}_2$  ( $20 \text{ mg (50 mL)}^{-1}$ ); (c), Ag(0.24 wt.%) $\text{TiO}_2$  ( $50 \text{ mg (50 mL)}^{-1}$ ). A mixture of acetonitrile and  $\text{H}_2\text{O}$  (1 : 99 v/v) was used as the solvent. The  $I_{320-400}$  was  $4.6 \text{ mW cm}^{-2}$ . B, The Arrhenius plots of  $\ln k$  vs.  $1000/T$  for Au(0.25 wt.%) $\text{TiO}_2$  (b) and Ag(0.24 wt.%) $\text{TiO}_2$  (c).

than for Ag(0.24 wt.%) $\text{TiO}_2$ . Also,  $E_a$  decreases with loading of Au by a factor of 1.6, whereas the Ag loading has no effect on it.

The strangest and most intriguing fact of this reaction is that RS adsorbed on Au desorbs from the surface upon irradiation despite its strong adsorption strength.<sup>11</sup> Scheme 2 depicts the energy diagrams in the Ag/ $\text{TiO}_2$  and Au/ $\text{TiO}_2$  system.<sup>19,27-30</sup> When metals are brought into contact with  $\text{TiO}_2$ , electron transfer occurs until the Fermi energies of both phases coincide. This Fermi energy after equilibrium ( $E_f$ ) is approximately equal to the Fermi energy of the metal, because metals have continuous electronic energy levels in an unfilled wide band. A couple of bonding and anti-bonding orbitals are formed as the result of interaction between the HOMO of the  $\text{RS}^-$  radical<sup>31</sup> and an unoccupied molecular orbital (UMO) above the  $E_f$  of Au (or Ag).<sup>32</sup> The MO calculation gave a value of  $-6.41 \text{ eV}$  for the HOMO energy of the  $\text{RS}^-$  radical.<sup>9</sup> In the ground state, the bonding orbital is occupied by two electrons, belonging originally to the  $\text{RS}^-$  radical and Au (or Ag), respectively, leading to a strong interfacial  $\text{RS-Au}$  (or  $\text{RS-Ag}$ ) bond. The contribution of the HOMO of the  $\text{RS}^-$  radical to the bonding orbital is much greater than that of the UMO of Au (or Ag). Then the interfacial bond can formally



**Scheme 2** Energy diagram of the reaction system. In constructing this, the following values were used: the work functions of Ag = 4.0 eV and Au = 5.1 eV;<sup>27</sup> the electron energy for the normal hydrogen electrode (NHE), -4.5 eV vs. NHE;<sup>28</sup> the flat band potential of TiO<sub>2</sub> at pH 5.5, -0.45 V from the vacuum level;<sup>29</sup> the band gap energy of TiO<sub>2</sub> (anatase), 3.2 eV;<sup>29</sup> the oxidation potential of H<sub>2</sub>O at pH 0, 1.23 V vs. NHE;<sup>29</sup> the highest occupied molecular orbital (HOMO) of RS, -6.4 eV.<sup>9</sup>

be described as RS<sup>-</sup>-Au<sup>+</sup> (or RS<sup>-</sup>-Ag<sup>+</sup>), which is confirmed by X-ray photoelectron spectroscopy measurements of SAMs.<sup>33</sup> On the other hand, in the photoexcitation state,  $E_f$  rises by several hundred meV ( $E'_f$ ),<sup>34</sup> which corresponds to the bonding energy of R'SSR' on Au (~0.5 eV per R'S group).<sup>35</sup> If  $E'_f$  exceeds the energy of the anti-bonding orbital ( $\psi_a$ ), it would be occupied by the two electrons from Au (or Ag). The destabilizing energy will enable desorption of RS<sup>-</sup> upon illumination, continuing the photocatalytic cycle in this reaction.

In the Ag/TiO<sub>2</sub> system, the  $E_f$  of Ag (4.0 ± 0.15 eV) is close to that of TiO<sub>2</sub> (ca. 4.0 eV) before illumination. As shown in Scheme 2, on illumination  $E_f$  increases evenly to a value of  $E'_f$ . In the Au/TiO<sub>2</sub> system, however, the  $E_f$  of Au (5.1 ± 0.1 eV) is much greater than of TiO<sub>2</sub>. Upon illumination, flattening of the band bending of TiO<sub>2</sub> takes place, followed by electron transfer from TiO<sub>2</sub> to Au. The electrons captured by Au should be transferred predominantly to  $\psi_a$ , which is situated well below the flat band potential of TiO<sub>2</sub>. Noticeably, the high work function of Au effectively inhibits back electron transfer from Au to the conduction band (CB) of TiO<sub>2</sub>, while it competes with electron transfer from the metal to  $\psi_a$  in the Ag/TiO<sub>2</sub> system. It follows that  $k_{d2}(\text{Au/TiO}_2) < k_{d2}(\text{Ag/TiO}_2)$ . The larger  $k$  value for the Au/TiO<sub>2</sub> system is thus ascribable to the increase in the efficiency of the charge separation, i.e., the increase in the term  $k_0[\text{H}_2\text{O}_{ad}]^{1/2}/(k_{d2} + k_0[\text{H}_2\text{O}_{ad}]^{1/2})$  in eqn. (3). This equation can further be rewritten as eqn. (6) by introducing a parameter  $r$  indicating the relative magnitude of  $k_{d2}$  to  $k_0$ .

$$k = (\text{other terms}) \times [\exp(-E_0/RT)/(\exp(-E_0/RT) + r \exp(-E_{d2}/RT))] \quad (6)$$

where  $E_0$  and  $E_{d2}$  are the activation energies of steps 6 and 5 in Scheme 1, respectively.

Approximation of the denominator of eqn. (6) by a function  $\exp[(-r/(r+1))(E_0 - E_{d2})/RT]$  leads to eqn. (7).

$$\ln k \sim (\text{other terms}) - [r/(r+1)][(E_0 - E_{d2})/RT] \quad (7)$$

Then, the apparent activation energy  $E_a$  is expressed as a function of  $r$ .

$$E_a \propto [r/(r+1)][(E_0 - E_{d2})/R] \quad (8)$$

Recombination of the photogenerated charge carriers is generally an ultra-fast process (<100 ns), which means that  $E_{d2}$  is very small or  $E_0 - E_{d2} > 0$ . Taking  $r(\text{Au/TiO}_2) < r(\text{Ag/TiO}_2)$  into consideration, the decrease in  $E_a$  with Au loading in place of Ag can be explained by eqn. (8).

## Conclusions

Nanometre-sized Au (4.3–11 nm) and Ag particles (<5 nm) were loaded onto the surface of TiO<sub>2</sub> by the deposition-precipitation method and the photodeposition method, respectively. TiO<sub>2</sub> photocatalytic reduction of bis(2-dipyridyl) disulfide to 2-mercaptopyridine by H<sub>2</sub>O was enhanced significantly with a small amount of Au ( $x \sim 0.3$  wt.%). The kinetic studies revealed that the rate constant of the Au/TiO<sub>2</sub> system is 2.6 times greater than of the Ag/TiO<sub>2</sub> system and the activation energy of the former is smaller than that of the latter by a factor of 1.6. This enhancing effect of Au could be attributed to the increase in the charge separation efficiency, which is achieved by restriction of back electron transfer due to the high work function of Au.

## Acknowledgements

The authors express sincere gratitude to Dr. Masatake Haruta and Dr. Susumu Tsubota (Osaka National Research Institute) for helpful comments on the deposition-precipitation method, Dr. Mitsunobu Iwasaki (Kinki University) for valuable discussion and Ishihara Techno Co. for the gift of the TiO<sub>2</sub> particles (A-100). Finally, the authors thank the two reviewers for constructive criticisms of an earlier version of this manuscript.

## References

- 1 Photocatalytic Purification and Treatment of Water and Air, ed., F. D. Allies and H. Al-Ekabi, Elsevier, Amsterdam, 1993.
- 2 Duonghong, J. Ramsden and M. Graetzel, *J. Am. Chem. Soc.*, 1982, **104**, 2977.
- 3 J. Muzyka and M. A. Fox, *J. Photochem. Photobiol. A*, 1991, **57**, 27.
- 4 L. Lin and R. R. Kuntz, *Langmuir*, 1992, **8**, 870.
- 5 M. J. Bahneman, J. Moenig and R. Chapman, *J. Phys. Chem.*, 1987, **91**, 3782.
- 6 W. Choi and M. R. Hoffmann, *Environ. Sci. Technol.*, 1995, **27**, 1646.
- 7 W. H. Glaze, J. F. Kenneke and J. L. Ferry, *Environ. Sci. Technol.*, 1993, **27**, 177.
- 8 F. Mahdavi, T. C. Bruton and Y. Li, *J. Org. Chem.*, 1993, **58**, 744.
- 9 H. Tada, K. Teranishi, Y.-I. Inubushi and S. Ito, *Chem. Commun.*, 1998, 2345.
- 10 E. Cadot, M. Lacroix, M. Breyse and E. Arretz, *J. Catal.*, 1996, **164**, 490.
- 11 A. Ulman, *Chem. Rev.*, 1996, **96**, 1533 and references therein.
- 12 Y.-I. Inubushi, PhD Thesis, Kinki University, 1995.
- 13 S. Tsubota, M. Haruta, T. Kobayashi, A. Ueda and Y. Nakahara, in *Preparation of Catalysts V*, ed., G. Poncelet, P. A. Jacobs, P. Grange and B. Delmon, Elsevier, Amsterdam, 1991.
- 14 H. Kozuka, *Proc. SPIE*, 1997, **3136**, 304.

- 15 Calculation of the  $S$  value for Au/TiO<sub>2</sub> by assuming hemispherical Au deposits gives an increase of *ca.* 2% as compared to the value for TiO<sub>2</sub>. Thus, the increase in  $S$  could not be attributed simply to the Au deposition. However, no unsupported Au particles were observed by TEM.
- 16 T. Ishida, S.-I. Yamamoto, W. Mizutani, M. Motomats, H. Tokumoto, H. Hokari, H. Azebara and M. Fujihira, *Langmuir*, 1997, **13**, 3261.
- 17 J. Y. Gui, F. Lu, D. A. Stern and A. T. Hubbard, *J. Electroanal. Chem.*, 1990, **292**, 245.
- 18 C.-J. Zhong and M. D. Porter, *J. Am. Chem. Soc.*, 1994, **116**, 11616.
- 19 H. Tada, K. Teranishi, Y.-I. Inubushi and S. Ito, *Langmuir*, 2000, **16**, 3304.
- 20 X.-L. Zhou, X.-Y. Zhu and J. M. White, *Surf. Sci. Rep.*, 1991, **13**, 73.
- 21 The irradiation in air yielded some oxidative products. Details of the TiO<sub>2</sub> photoinduced oxidation of RSSR under aerated conditions will be reported elsewhere.
- 22 B. Gu, J. Kiwi and M. Graetzel, *Nouv. J. Chim.*, 1985, **9**, 539.
- 23 M. Haruta and S. Tsubota, *Catal. Catal.*, 1991, **33**, 440.
- 24 P. T. Landsberg, *Recombination in Semiconductors*, Cambridge University Press, Cambridge, 1991.
- 25 Step 6 can be divided further into the following elementary steps:
- $$\text{H}_2\text{O} \leftrightarrow \text{H}^+ \text{OH}^-$$
- $$\text{OH}_{\text{ad}}^- + \text{h}^+ \rightarrow \cdot\text{OH}$$
- $$2\cdot\text{OH} \rightarrow \text{H}_2\text{O}_2 \rightarrow \text{H}_2\text{O} + 1/2\text{O}_2$$
- For detailed information, see: J. Kiwi, K. Kalyanasundaram and M. Graetzel, *Struct. Bonding (Berlin)*, 1982, **49**, 39.
- 26 Another route for the RSH formation is possible.
- $$\text{H}^+ + \text{e}^- \rightarrow \text{H}_{\text{ad}}\cdot$$
- $$\text{H}_{\text{ad}}\cdot + \text{RS-M} \rightarrow \text{RSH} + \text{M}$$
- However, we confirmed that the back reaction occurs in the dark, *i.e.*, the addition of an authentic RSH sample to a suspension of Au/TiO<sub>2</sub> particles produces H<sub>2</sub> followed by preferential adsorption of RS groups on the Au surfaces. Thus, this possibility seems to be small.
- 27 D. E. Eastman, *Phys. Rev. B*, 1970, **2**, 1.
- 28 F. Z. Lohaman, *Naturforsch. A*, 1967, **22**, 843.
- 29 M. Graetzel, in *Energy Resources through Photochemistry and Catalysis*, ed. M. Graetzel, Academic Press, New York, 1983.
- 30 The HOMO energy of the RS<sup>·</sup> radical was obtained by PM3 MO calculations (for details see ref. 19). For thiols, two types of dissociative adsorption of the S-H bond on coinage metals (M) were proposed (eqn. (a) and (b)).
- $$\text{R'SH} + \text{M}(\text{o}) \rightarrow \text{R'S}^-\text{M}(\text{i}) + 1/2\text{H}_2 \quad (\text{a})$$
- $$\text{R'SH} + \text{M}(\text{i}) \rightarrow \text{R'S}^-\text{M}(\text{i}) + \text{H}^+ \quad (\text{b})$$
- see: P. E. Laibinis, G. M. Whitesides, D. L. Allara, Y.-T. Tao, A. N. Parikh and R. G. Nuzzo, *J. Am. Chem. Soc.*, 1991, **113**, 7152. However, the homolytic dissociative adsorption corresponding to eqn. (a) seems to be plausible in the case of disulfides (eqn. (c)).
- $$\text{R'SSR}' + \text{M}(\text{o}) \rightarrow 2\text{R'S}^-\text{M}(\text{i}) \quad (\text{c})$$
- 31 R. Hoffmann, *A Chemist's View of Bonding in Extended Structures*, VCH, New York, 1993.
- 32 G. K. Jennings and P. E. Laibinis, *J. Am. Chem. Soc.*, 1997, **119**, 5208.
- 33 T. Sakata, T. Kawai and K. Hashimoto, *Chem. Phys. Lett.*, 1982, **88**, 50.
- 34 J. B. Schlenoff, M. Li and H. Ly, *J. Am. Chem. Soc.*, 1995, **117**, 12528.